

Elastic and electronic properties of fluorite RuO₂ from first principle

Z.J. Yang^{1*}, A.M. Guo², Y.D. Guo³, J. Li⁴, Z. Wang⁴, Q. Liu⁵, R.F. Linghu⁶, X.D. Yang⁷

¹ School of Science, Zhejiang University of Technology, Hangzhou 310023, China

² Department of Physics, California State University, Northridge, California 91330–8268, USA

³ School of Physics, Neijiang Normal University, Neijiang 641112, China

⁴ College of Material and Chemical Engineering, Hainan Provincial Key Laboratory of Research on Utilization of Si-Zr-Ti Resources, Hainan University, Haikou 570228, China

⁵ School of Physics, Chongqing University of Technology, Chongqing 400050, China

⁶ School of Physics, Guizhou Normal University, Guiyang 550001, China

⁷ Institute of Atomic and Molecular Physics, Sichuan University, Chengdu 610065, China

Received May 2, 2011, in final form February 1, 2012

The elastic, thermodynamic, and electronic properties of fluorite RuO₂ under high pressure are investigated by plane-wave pseudopotential density functional theory. The optimized lattice parameters, elastic constants, bulk modulus, and shear modulus are consistent with other theoretical values. The phase transition from modified fluorite-type to fluorite is 88 GPa (by localized density approximation, LDA) or 115.5 GPa (by generalized gradient approximation, GGA). The Young's modulus and Lamé's coefficients are also studied under high pressure. The structure turned out to be stable for the pressure up to 120 GPa by calculating elastic constants. In addition, the thermodynamic properties, including the Debye temperature, heat capacity, thermal expansion coefficient, Grüneisen parameter, and Poisson's ratio, are investigated. A small band gap is found in the electronic structure of fluorite RuO₂ and the bandwidth increases with the pressure. Also, the present mechanical and electronic properties demonstrate that the bonding nature is a combination of covalent, ionic, and metallic contributions.

Key words: *first principle, electronic structure, elasticity, thermodynamicity*

PACS: 63.20.dk, 71.20.-b, 62.20.D-, 65.40.-b

1. Introduction

Attractions to study RuO₂ are due to its fundamental properties and potential superhard characteristics [1, 2]. An extensive search for new superhard materials has been undertaken during recent years and a new class of hard materials has been suggested: the transition-metal dioxides containing heavy elements. Typically, the bulk modulus of modified fluorite (pyrite phase, $Pa\bar{3}$) RuO₂ was found to be 399 GPa [3], which is the highest value except for diamond (442 GPa) [4]. RuO₂ has the rutile ($P4_2/mnm$) structure under usual conditions [3], and can be transformed to an orthorhombic ($CaCl_2$ -type, $Pnmm$) structure at about 6 GPa [5] or 11.8 GPa [6] and to a pyrite structure at about 12 GPa [2, 5]. Moreover, the theory indicates the $Pa\bar{3}$ structure can be transformed to a fluorite ($Fm\bar{3}m$) structure at about 89 GPa or 97 GPa [2].

Recently, elastic properties focusing on $Pa\bar{3}$ phase of RuO₂ have been investigated systematically [2, 7]. Electronic structures [8–11] and optical properties [12–14] of rutile and orthorhombic [14] RuO₂ have been extensively studied. A full-potential linear muffin-tin orbital calculation on the electronic structure and bulk modulus of fluorite RuO₂ has also been performed [15]. The hardness and elasticity in cubic RuO₂ and Raman scattering of the rutile-to- $CaCl_2$ phase transition have been probed experimentally [16].

*E-mail: yzjscu@163.com, Tel: 86 28 85405526, Fax: 86 28 85405515

Previous investigations on fluorite RuO₂ are not complete and some problems remain unresolved. Many properties, such as the hardness, stabilization, elastic and thermodynamic properties *etc* under high pressure, are still unknown. To reveal the superhard characteristics appropriately, a detailed theoretical description of the elastic and electronic properties is necessary.

2. Theoretical approaches

In this work, all the calculations have been performed with CASTEP [17, 18]. In the electronic structure calculations, we have used the non-local ultrasoft pseudopotential [19], together with the revised Perdew-Burke-Ernzerhof (RPBE) generalized gradient approximation (GGA) exchange-correlation function [20]. Considering the computational cost, a plane-wave basis set with an energy cut-off of 600.0 eV [2] has been applied, and the $12 \times 12 \times 12$ Monkhorst-Pack mesh has been used for the Brillouin-zone (BZ) k -point sampling. Pseudo atomic calculations have been performed for Ru ($4s^2 4p^6 4d^7 5s^1$) and O ($2s^2 2p^4$), where the self-consistent convergence of the total energy is at 5.0×10^{-7} eV/atom.

3. Results and discussion

In the equilibrium geometry calculations of fluorite RuO₂, both the GGA and the LDA methods have been used. The bulk modulus (B_0) and its first-order pressure derivative (B'_0) by Murnaghan [21] equation of state are listed in table 1.

Table 1. The calculated lattice constants a (Å), phase transition pressure P_t (GPa) and elastic constants c_{11} , c_{44} , c_{12} (GPa) by LDA and GGA methods at 0 GPa and 0 K. The bulk modulus B and shear modulus G are calculated by the elastic constants. The bulk modulus B_0 (GPa) and its first-order pressure derivatives B'_0 are fitted by the Murnaghan equation of state.

	a	B_0	B'_0	P_t	c_{11}	c_{44}	c_{12}	B	G
LDA (present)	4.7349	353	4.13	88	680.26	209.87	175.36	343.66	225.98
GGA (present)	4.8584	287	3.77	115.5	569.09	170.20	117.35	267.93	198.16
(LDA+GGA)/2	4.7967	320	3.95	102	624.68	190.04	146.36	305.79	212.07
[1, 22]		345		65					
[2]	4.743	384,351	3.5,4.2	89					
[2]	4.842	336,297	3.5,4.1	97	435	152	227		133
[15]		343							
[23]	4.842	328	4.2		410.6	62	286.6		62

The LDA/CAPZ (embedded in CASTEP) calculations are performed using the same parameter input with GGA.

Figure 1 suggests that a significant stiffer compressibility of 82.92% is obtained using LDA at 100 GPa as compared to GGA (80.27%). The volume compressibility (about 80%) is nearly the same as the ultra-stiff cubic TiO₂ at the same pressure [24]. The bulk modulus of the fluorite RuO₂ is 353 GPa (LDA) or 287 GPa (GGA), which is slightly smaller than that of the TiO₂ (282 GPa ÷ 395 GPa). As the pressure is increased to 100 GPa, the approximation value of the normalized volume of diamond, *c*-BN, OsO₂, and OsC, is 85%, 83%, 80%, and 84%, respectively [25–27], which is slightly larger than the current calculations. As a comparison, figure 1 shows the Ru-O bond length contraction with increasing the pressure. Similarly, a smaller Ru-O bond length contraction is obtained using LDA. In a word, the current Ru-O bond length contraction, using either LDA or GGA, is much smaller than that in volume contraction.

The calculated elastic constants of fluorite RuO₂ under different pressures are listed in table 2. According to the generalized elastic stability criteria [28] ($c_{11} - c_{12} > 0$, $c_{11} + 2c_{12} > 0$, $c_{44} > 0$) for cubic crystals, we can demonstrate that fluorite structure is elastic stable under 120 GPa. The larger c_{11} and smaller c_{12} indicate the inter-atomic bonding along the *c*-axis stronger than that along the *a*-axis, consistent with the case of the larger bulk modulus B and the smaller shear modulus G over a wide pressure

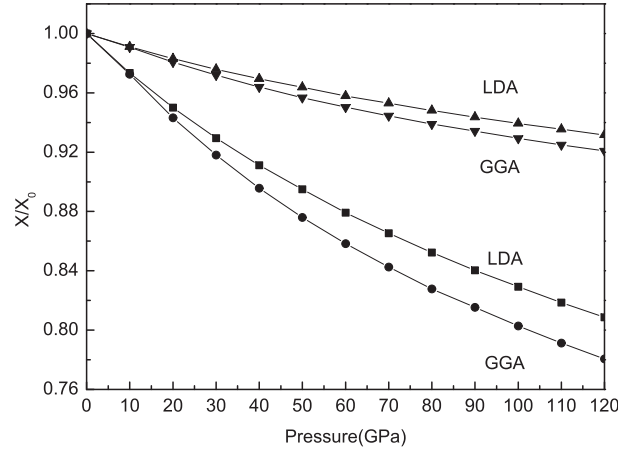


Figure 1. Variation of the lattice volume (denoted by square and circle symbols) and the Ru-O bond length (denoted by triangle symbols) with pressure. They are normalized by X/X_0 , where X and X_0 are the lattice volume or Ru-O bond length at any given pressure and zero pressure at zero temperature.

range. Compared to c_{12} and c_{44} , c_{11} varies largely by changing the pressure, meaning that it is more difficult to obtain the same strain from the longitudinal direction than from the transverse direction.

An estimate of the zero-temperature transition pressure between the $Pa\bar{3}$ and $Fm\bar{3}m$ structures may be obtained from the usual condition of equal enthalpies, i.e., the pressure P , at which enthalpy $H = E + PV$ of both phases is the same. Our calculated $Pa\bar{3} \rightarrow Fm\bar{3}m$ phase transition pressure is 115.5 GPa by GGA and 88 GPa by LDA, as shown in figure 2, in accordance with the theoretical values of 89 GPa [2] and 97 GPa [2] but is greater than the predicted 65 GPa [1, 22].

Using the calculated elastic constants at 0 K and 0 GPa, we obtain the bulk moduli B of fluorite RuO₂, with the values of 287 GPa (GGA) and 353 GPa (LDA), respectively, which is smaller than that of diamond (442 GPa [27]), although both of them have comparable compressibility at 100 GPa. The shear constant c_{44} is 170.20 GPa (GGA), which is consistent with previous theoretical calculations 152 GPa [2], 140 GPa [16], 147 GPa [16], and experimental measurement 144 GPa [16], but is larger than the other theoretical value 62 GPa [23]. In general, the shear modulus of cubic materials is slightly lower than the value of c_{44} [16], whereas our calculation indicates the opposite case.

There have been proposals that the shear modulus may be a better index of hardness [29]. Our calcu-

Table 2. The calculated (by GGA method) elastic constants c_{11} , c_{44} , c_{12} (GPa), heat capacity C_V ($J \cdot mol^{-1} \cdot K^{-1}$), Debye temperature Θ (K), Grüneisen parameter γ , thermal expansion coefficient α ($10^{-5} K^{-1}$) and Poisson's ratio σ over a wide pressure range at zero temperature.

P	V/V_0	c_{11}	c_{44}	c_{12}	C_V	Θ	γ	α	σ
0	1	569.0981	170.2064	117.3517	47.1572	872.0784	0.7086	4.3589	0.2124
10	0.9725	618.5525	182.6494	142.5632	42.9681	905.9000	0.6871	3.5224	0.2247
20	0.9432	672.0389	203.7597	177.3234	37.9710	948.9614	0.6643	2.7310	0.2351
30	0.9719	724.0007	214.6731	213.0271	34.9787	976.2347	0.6447	2.2390	0.2498
40	0.8957	780.0562	227.5737	254.8032	32.0164	1004.6197	0.6276	1.8230	0.2638
50	0.8759	832.5314	239.1418	287.9699	29.2934	1031.9559	0.6124	1.5240	0.2724
60	0.8583	882.1365	250.6513	326.8776	27.0493	1055.4048	0.5989	1.2880	0.2820
70	0.8426	928.6125	258.9245	359.1524	25.1941	1075.4502	0.5870	1.1170	0.2894
80	0.8278	985.5626	273.7571	401.9691	22.7703	1103.0287	0.5757	0.9278	0.2965
90	0.8153	1024.6117	279.8891	438.2222	21.7231	1115.3097	0.5663	0.8321	0.3043
100	0.8027	1066.3426	285.4165	469.7282	20.5262	1129.5911	0.5568	0.7442	0.3102
110	0.7913	1111.9641	294.8567	508.1361	19.1198	1146.9061	0.5482	0.6525	0.3159
120	0.7806	1156.7986	294.2600	540.1705	18.4615	1154.9119	0.5401	0.5986	0.3227

lated values of G , 225.98 GPa by LDA and 198.16 GPa by GGA, are much greater than the theoretical values of 133 GPa [2] and 62 GPa [23]. Even so, the current results are still incomparable with those of diamond and c -BN, e.g., the recently calculated values for diamond are 550 GPa [30], 545 GPa [31], 518 GPa [31], and 403 GPa for c -BN [30]. However, the current results are comparable to those of OsO_2 [31] with values of 250 GPa (LDA) and 223 GPa (GGA) ([15] suggests OsO_2 as a better candidate for a hard material since their calculations confirmed that the bulk modulus of OsO_2 , 452 GPa, is only smaller than that of diamond). Overall, it is reasonable to suggest that the fluorite RuO_2 is a potential ultra-incompressible material, consistent with the suggest superhard material from [2].

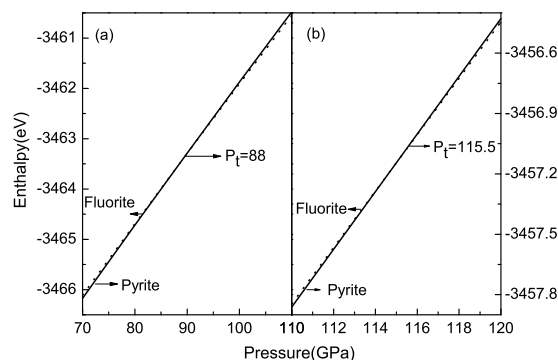


Figure 2. Enthalpy as a function of pressures for the $Pa\bar{3}$ and $Fm\bar{3}m$ phases of RuO_2 , (a) is the LDA results and (b) is GGA ones.

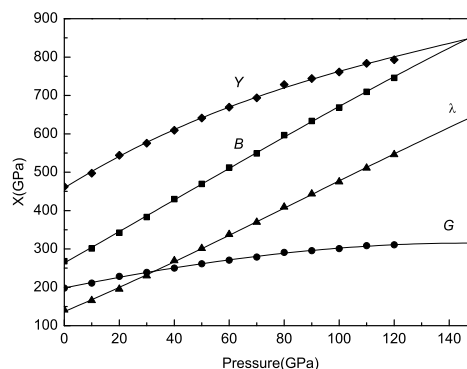


Figure 3. Pressure dependences of mechanical quantities (by GGA method) under different pressures, X represents Bulk modulus B , Shear modulus G , Young's modulus Y , Lamé's coefficients λ .

In order to better understand the pressure responses of the mechanical behavior, we have studied the bulk modulus B , shear modulus G , Young's modulus Y , and Lamé's coefficients λ by increasing the pressure to 150 GPa. The Young's modulus Y and Lamé's coefficients λ are also essential for understanding the macroscopic mechanical properties of solids and for designing hard materials. Figure 3 shows the most significant pressure dependence of B and the least significant pressure dependence of G . In contrast to B , the Lamé's coefficients λ increase slowly with pressure. Compared to Lamé's coefficients λ , the Young's modulus Y behaves much slower with the increase of pressure. At zero pressure, the relative magnitude of the four mechanical parameters in descending order is: $Y > B > G > \lambda$. However, the Lamé's coefficient λ is larger than G above nearly 30 GPa, and the B is larger than Y above nearly 150 GPa. The high Y and B , particularly at high pressures, also suggest that fluorite RuO_2 is a potential ultrahard material.

The value of the Poisson's ratio for covalent materials is small ($\sigma = 0.1$), whereas for ionic materials, a typical value of σ is 0.25 [32]. In our cases, the value of σ for RuO_2 varies from about 0.2124 to 0.3227, as shown in table 2, indicating a higher ionic and weaker covalent contribution to intra-atomic bonding. Besides, the typical relation between bulk and shear modulus is, respectively, $G \approx 1.1B$ and $G \approx 0.6B$ for covalent and ionic materials. In our cases, the calculated values of G/B are in the range of 0.7396 at 0 GPa to 0.3656 at 150 GPa, indicating that the ionic bonding is dominant for fluorite RuO_2 . To evaluate the material ductility or brittleness, Pugh *et al.* introduced the B/G ratio [33]: the material is brittle if the ratio is less than the critical value 1.75. Therefore, fluorite RuO_2 is brittle under ambient conditions since the B/G is only 1.35. However, the brittleness decreases (or ductility increases) when the pressure is increased and the B/G ratio rises to 2.4 when the pressure is up to 120 GPa.

The dependences of the Debye temperature Θ , heat capacity C_V , Grüneisen parameter γ , thermal expansion coefficient α , and Poisson's ratio σ on the pressure are calculated. As shown in table 2, when the temperature keeps constant ($T = 0$ K), Θ and σ increase with increasing the pressure, whereas C_V , γ , and α decrease. The five thermodynamic parameters show different pressure dependences within the range of 0 ÷ 120 GPa. It is obvious that the thermal expansion coefficient α declines most significantly, corresponding to an 85% compression. The heat capacity C_V and Grüneisen parameter γ , however, correspond to smaller compressions with 60% and 25%, respectively. The other two parameters, Debye temperature

Θ and Poisson's ratio σ , increase with the pressure with 32% and 52%, respectively. Moreover, all the five parameters have shown decreased dependences with increasing the pressure, indicating anharmonicity of the vibration. Therefore, it is necessary to further investigate the electronic energy band structure and density of states (DOS) to better understand the physical properties. Accordingly, we have made a systematic investigation of the fluorite RuO₂ at different pressures (0, 30, 60, 90 GPa) under 0 K, as shown in figures 4, 5, and 6.

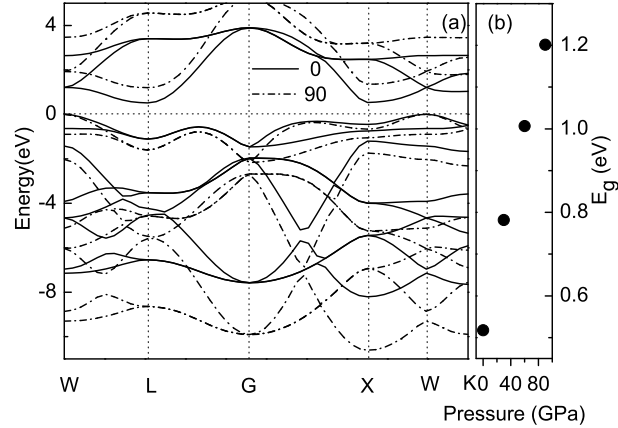


Figure 4. Energy band structure (by GGA method) along the high symmetry points in the Brillouin zone at the pressures of 0, 90 GPa is shown in (a) and the band gap E_g as a function with the applied pressures is shown in (b).

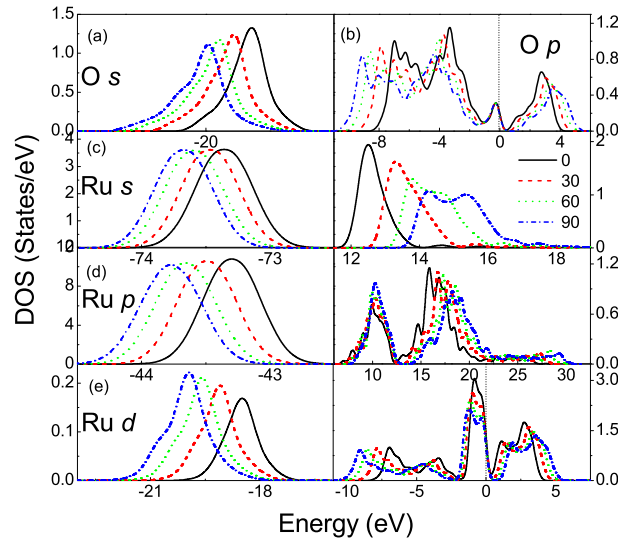


Figure 5. (Color online) Partial density of states (by GGA method) of O and Ru states under $P = 0, 30, 60, 90$ GPa.

Figure 4 presents the pressure-induced energy level shift towards higher and lower regions. We can see that the applied pressure has a larger effect on the energy levels far away from the Fermi level than those in the vicinity of the Fermi level, indicating a stronger effect on the core level than on the valence level. From the energy band structure, we find that the top of the valence band occurs at W point and the bottom of the conduction band occurs at L point (slightly lower than X point by a value of 0.02 eV), implying that there exists an indirect gap with width of 0.5175 eV in fluorite RuO₂. The calculated band gap at zero pressure is consistent with the other theoretical value (0.5 eV) [2], but is much smaller than those of diamond (4.15 eV) and c -BN (4.49 eV) [34]. Moreover, it is found that the band gap increases almost linearly with the pressure.

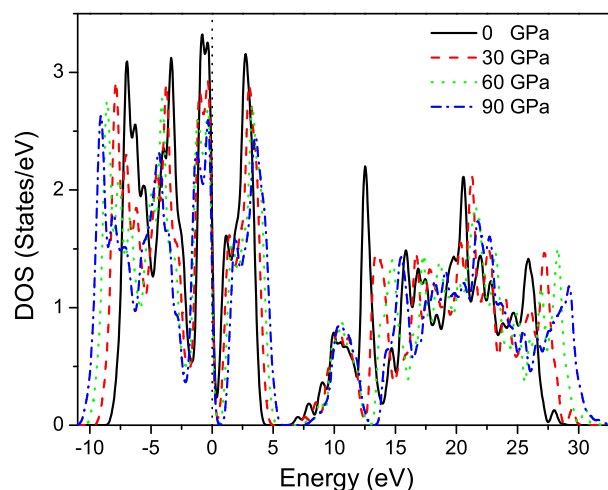


Figure 6. (Color online) Total density of states (by GGA method) under $P = 0, 30, 60, 90$ GPa near the Fermi level.

In figures 5 and 6, we plot the calculated DOS by GGA, where the Fermi energy is taken to be zero. From figure 5 (a), the O $2s$ band center is at -18.5 eV, which is consistent with those in rutile [10, 14] and CaCl_2 -type [14] RuO_2 . The valence band width is about 4 eV, which is much larger than those in rutile [14] (2.5 eV) and CaCl_2 -type [14] RuO_2 (1.4 eV). In figure 5 (b), the calculated valence band width of O $2p$ is about 8 eV, which is slightly larger than that in rutile RuO_2 of 5.9 eV (using an extended linear augmented plane wave potential) and 6.8 eV (using linear-muffin-tin-orbital potential) [10], but the present calculation is consistent with that in rutile [14] and CaCl_2 -type [14] RuO_2 with the same values of about 8.1 eV. Furthermore, the calculated conduction band width is 4 eV, which is far smaller than that of valence conduction.

The Ru s semi-core band, centered at -73.3 eV, displays larger relative intensity (3.6) and smaller width (1.2 eV) with respect to those in the conduction band with smaller relative intensity (1.9) and larger width (2.2 eV). The other Ru s electrons distribute mainly in the ranges of -21 eV \div -18 eV, -8.6 eV \div -1.6 eV, -1.5 eV \div 0.5 eV, have formed very weak peak with intensities less than 0.1, and thus could be ignored as compared with the peak far away from the Fermi level. In figure 5 (d), the Ru p state locates at -43.5 eV in the valence band with width of 1.3 eV and distributes in the energy range of $6.3 \div 27.5$ eV in the conduction band (corresponding to two sharp peaks centered at around 10 eV and 16 eV, respectively). The relative intensity of Ru p state in the valence band is far greater than that in conduction band, and the DOS distributed in the energy range $-20 \div 5$ eV is ignored due to their subtle relative intensities (below 0.12). The Ru $4d$ state, shown in figure 5 (e), is distributed at -18.8 eV and around the Fermi level with widths of 2.3 eV and 12.0 eV, respectively. Moreover, the relative intensity of the inner valence band is considerably smaller than that in the outer valence band and in the conduction band.

The four sharp peaks of the total DOS within $-7.5 \div 5$ eV originate from the strong hybridization between Ru $4d$ and O $2p$, as seen in figure 6. The complete overlap of the Ru $4d$ and O $2p$ states from -8 eV to 4 eV indicates a strong covalent interaction between them, whereas the nonzero DOS value at Fermi level indicates a moderate metallic feature in its bonding state. Although there is a large hybridization between Ru $4d$ and O $2p$ states, the charge transfer from Ru to O is possible in the present case. By analyzing the Mulliken population results, it is found that the charge transfer from Ru to O is as numerous as about 1.01 electrons. Therefore, the bonding behavior between Ru-O has ionic contributions owing to charge transfer. In a word, the bonding behavior between the Ru-O is a combination of covalent, metallic and ionic contributions.

To emphasize the pressure dependence of the DOS, we have investigated the DOS under different pressures (30, 60, 90 GPa), as shown in figures 5 and 6. It is clearly seen that the applied pressure causes the energy levels shifting towards both sides of the Fermi level and thus the energy band is broadened. Under a higher pressure, the energy level shift is decreased, implying the strong repulsion among the

core electrons. Meanwhile, in general, the relative intensity decreases with increasing the pressure. Accordingly, the relative shift in the lower energy space is always larger than those in the higher energy space, implying different bonding strength. The change of the DOS can be attributed to the charge transfer during lattice distortion. With the increase of pressure, a higher overlap of the wavefunction results in a stronger delocalization of electrons. Electrons transfer from the majority to minority spin band and form broader bands. The center changes and electrons become more localized when lattice distortion changes from negative to positive. The majority and minority bands move with respect to the Fermi level, which affects both the spin polarization ratio and magnetic properties. The current investigations reveal that the relative intensity of O *s* and *p* states decrease with the pressure both in the valence and conduction bands. However, the relative intensity of Ru *s* state keeps almost unchanged in the semi-core band and the main peak in the conduction band has been split into two peaks with the pressure. By analyzing Ru *p* state, we find that the relative intensity decreases slightly with the pressure in the whole valence band and in the higher-energy range from 12.5 eV to 25 eV, but increases with the pressure within 7.5 eV÷12.5 eV. Interestingly, there is observed an increase of the relative intensity of Ru *d* state with the pressure in the deeper-lying valence band, whereas the relative intensity of the other Ru *d* state decreases with the pressure, presenting opposite variation tendencies. The different intensity variation trends have unambiguously demonstrated that the applied pressure has induced various charge transfer tendencies.

4. Conclusions

The current investigations revealed that the fluorite RuO₂ is a potential ultrahard material. The elastic stability criteria show that the fluorite RuO₂ is elastic stable up to 120 GPa. The calculated Poisson's ratio and Debye temperature increase monotonously with the pressure. However, the heat capacity, Grüneisen parameter, and thermal expansion coefficient decrease with the pressure. An analysis based on Poisson's ratio, G/B , and DOS reveals that the bonding nature in RuO₂ is a combination of ionic, covalent and metallic contributions, which contributes to the hardness and fundamental properties. The energy band investigations found an energy gap between the top of the valence band and the bottom of the conduction band, and the gap seems to increase monotonously with the pressure. Moreover, the different intensity variation trends of DOS have unambiguously demonstrated that the applied pressure has caused various charge transfer tendencies.

Acknowledgements

We are thankful for financial support from the National Natural Science Foundation of China (Grant Nos: 10974139, 10964002, 11104247) and the Provincial Natural Science Foundation of Guizhou (Grant Nos: [2009]2066 and TZJF-2008-42), Hainan (Grant No: 110001), Chong Qing (Grant No: CSTCstc2011jja90002) and Zhejiang (Grant No: Y201121807).

References

1. Hugosson H.W., Grechnev G.E., Ahjua R., Helmersson U., Sa L., Eriksson O., Phys. Rev. B, 2002, **66**, 174111; doi:10.1103/PhysRevB.66.174111.
2. Tse J.S., Klug D.D., Uehara K., Li Z.Q., Phys. Rev. B, 2000, **61**, 10029; doi:10.1103/PhysRevB.61.10029.
3. Haines J., Leger J.M., Shulte O., Science, 1996, **271**, 629; doi:10.1126/science.271.5249.629.
4. Aleksandrov I.V., Goncharov A.F., Zisman A.N., Stishov S.M., Zh. Eksp. Teor. Fiz., 1987, **93**, 680 (in Russian) [Sov. Phys. JETP, 1987, **66**, 384].
5. Haines J., Leger J.M., Phys. Rev. B, 1993, **48**, 13344; doi:10.1103/PhysRevB.48.13344.
6. Rosenblum S.S., Weber W.H., Phys. Rev. B, 1997, **56**, 529; doi:10.1103/PhysRevB.56.529.
7. Yang Z.J., Guo Y.D., Wang G.C., Li J., Dai W., Liu J.C., Cheng X.L., Yang X.D., Chin. Phys. B, 2009, **18**, 4981; doi:10.1088/1674-1056/18/11/061.
8. Glassford K.M., Chelikowsky J.R., Phys. Rev. B, 1993, **47**, 1732; doi:10.1103/PhysRevB.47.1732.
9. Yang Z.J., Guo Y.D., Li J., Liu J.C., Dai W., Cheng X.L., Yang X.D., Chin. Phys. B, 2010, **19**, 077102; doi:10.1088/1674-1056/19/7/077102.

10. Yavorsky B.Y., Krasovska O.V., Krasovskii E.E., Yaresko A.N., Antonov V.N., *Physica B*, 1996, **225**, 243; doi:10.1016/0921-4526(96)00270-0.
11. Glassford K.M., Chelikowsky J.R., *Phys. Rev. B*, 1994, **49**, 7107; doi:10.1103/PhysRevB.49.7107.
12. De Almeida J.S.D., Ahuja R., *Phys. Rev. B*, 2006, **73**, 165102; doi:10.1103/PhysRevB.73.165102.
13. Daniels R.R., Margaritondo G., *Phys. Rev. B*, 1984, **29**, 1813; doi:10.1103/PhysRevB.29.1813.
14. Benyahia K., Nabi Z., Tadjer A., Khafi A., *Physica B*, 2003, **339**, 1; doi:10.1016/S0921-4526(03)00417-4.
15. Lundin U., Fast L., Nordstrom L., Johansson B., *Phys. Rev. B*, 1998, **57**, 4979; doi:10.1103/PhysRevB.57.4979.
16. Leger J.M., Djemia P., Ganot F., Haines J., Pdereira A.S., Jormada J.A.H., *Appl. Phys. Lett.*, 2001, **79**, 2169; doi:10.1063/1.1401786.
17. Payne M.C., Teter M.P., Allen D.C., Arias T.A., Joannopoulos J.D., *Rev. Mod. Phys.*, 1992, **64**, 1045; doi:10.1103/RevModPhys.64.1045.
18. Milman V., Winkler B., White A., Packard C.J., Payne M.C., Akhmatkaya E.V., Nobes R.H., *Int. J. Quantum Chem.*, 2000, **77**, 895; doi:10.1002/(SICI)1097-461X(2000)77:5<895::AID-QUA10>3.0.CO;2-C.
19. Vanderbilt D., *Phys. Rev. B*, 1990, **41**, 7892; doi:10.1103/PhysRevB.41.7892.
20. Hammer B., Hansen L.B., Norskov J.K., *Phys. Rev. B*, 1999, **59**, 7413; doi:10.1103/PhysRevB.59.7413.
21. Murnaghan F.D., *Proc. Natl. Acad. Sci. U.S.A.*, 1944, **30**, 244; doi:10.1073/pnas.30.9.244.
22. Ahuja R., Rekhi S., Saxena S.K., Johansson B., *J. Phys. Chem. Solids*, 2001, **62**, 2035; doi:10.1016/S0022-3697(01)00049-X.
23. Sekkal W., Zaoui A., *J. Phys.: Condens. Matter*, 2001, **13**, 3699; doi:10.1088/0953-8984/13/16/301.
24. Swamy V., Muddle B.C., *Phys. Rev. Lett.*, 2007, **98**, 035502; doi:10.1103/PhysRevLett.98.035502.
25. Zheng J.C., *Phys. Rev. B*, 2005, **72**, 052105; doi:10.1103/PhysRevB.72.052105.
26. Knittle E., Wentzcovich R.M., Jeanloz R., Cohen M.L., *Nature*, 1989, **337**, 349; doi:10.1038/337349a0.
27. McSkimin H.J., Bond W.L., *Phys. Rev.*, 1957, **105**, 116; doi:10.1103/PhysRev.105.116.
28. Wang J.H., Yip S., Phillpot S., Wolf D., *Phys. Rev. B*, 1995, **52**, 12627; doi:10.1103/PhysRevB.52.12627.
29. Teter D.M., *MRS Bull.*, 1998, **23**, 1.
30. Liang Y.C., Zhang B., *Phys. Rev. B*, 2007, **76**, 132101; doi:10.1103/PhysRevB.76.132101.
31. Fan C.Z., Zeng S.Y., *Phys. Rev. B*, 2006, **74**, 125118; doi:10.1103/PhysRevB.74.125118.
32. Haines J., Leger J.M., Bocquillon G., *Annu. Rev. Mater. Res.*, 2001, **31**, 1; doi:10.1146/annurev.matsci.31.1.1.
33. Pugh S.F., *Philos. Mag.*, 1954, **45**, 833.
34. Luo X.G., Guo X.J., Liu Z.Y., He J.L., Yu D.L., Xu B., Tian Y.J., *Phys. Rev. B*, 2007, **76**, 092107; doi:10.1103/PhysRevB.76.092107.

Пружні та електронні властивості флюориту RuO₂ з перших принципів

З.Дж. Янг¹, А.М. Гуо², Й.Д. Гуо³, Дж. Лі⁴, З. Ванг⁴, К. Ліу⁵, Р.Ф. Лінгха⁶, Х.Д. Янг⁷

¹ Природничий факультет, Технологічний університет Чжецзяну, 310023 Ханчжоу, КНР

² Фізичний факультет, Каліфорнійський державний університет, Нортрідж, Каліфорнія 91330-8268, США

³ Фізичний факультет, Педагогічний університет Нейцзяну, Нейцзян 641112, КНР

⁴ Коледж матеріалознавства і хімічної інженерії, Хайнанська центральна регіональна дослідна лабораторія з питань утилізації Si-Zr-Ti, Хайнанський університет, Хайкоу 570228, КНР

⁵ Фізичний факультет, Чунцинський технологічний університет, Чунцин 400050, КНР

⁶ Фізичний факультет, Педагогічний університет Гуйчжоу, Гуйян 550001, КНР

⁷ Інститут атомної і молекулярної фізики, Сичуанський університет, Ченду 610065, КНР

Пружні, термодинамічні та електричні властивості флюориту RuO₂ при високому тиску досліджуються за допомогою теорії функціоналу густини з плоскохвильовим псевдопотенціалом. Оптимізовані параметри ґратки, пружні сталі, об'ємний модуль і модуль зсуву узгоджуються з іншими теоретичними значеннями. Фазовий перехід з модифікованого флюориту до флюориту є при 88 GPa (наближення локальної густини, LDA), чи при 115.5 GPa (узагальнене градієнтне наближення, GGA). Також досліджено модуль Юнга і коефіцієнти Ламе при високих тисках. Структура є стабільною для тисків до 120 GPa, якщо обчислювати пружні сталі. Крім того, досліджено термодинамічні властивості, включаючи температуру Дебая, теплоємність, коефіцієнт теплового розширення, параметр Грюнайзена і коефіцієнт Пуассона. В електронній структурі флюориту RuO₂ знайдено малу зонну щілину і ширина зони зростає із тиском. Також, представлені механічні та електронні властивості демонструють, що природа зв'язування є комбінацією ковалентного, іонного і металічного вкладів.

Ключові слова: перші принципи, електронна структура, пружність, термодинамічність
